Osaka University Knowledge Archive

Title	Weldability of 18%Ni Maraging Steel (HT 210) by Ultra High Voltage Electron Beam Welding(Materials, Metallurgy & Weldability)
Author(s)	Arata, Yoshiaki; Tomie, Michio; Katayama, Seiji
Citation	Transactions of JWRI. 1985, 14(1), p. 97-106
Version Type	VoR
URL	https://doi.org/10.18910/3680
rights	
Note	

Osaka University Knowledge Archive : OUKA

https://ir.library.osaka-u.ac.jp/

Osaka University

Weldability of 18%Ni Maraging Steel (HT 210) by Ultra High Voltage Electron Beam Welding†

Yoshiaki ARATA*, Michio TOMIE** and Seiji KATAYAMA***

Abstract

A study was conducted for the applicability of a 250 kV ultra high voltage electron beam of an ultra high energy density heat source to the flat position full penetration welding of 12.8 mm thick plates of 18%Ni maraging steel (HT 210). It was verified that this ultra high voltage welding was advantageous to the production of a sound narrow weld bead without weld defects such as porosity, etc. Moreover, investigation of the effect of heat treatments on the mechanical properties of electron beam weld metals revealed an optimum combination of both homogenization and grain-refining solution heat treatments to achieve the highest hardness, strength and fracture toughness of the weld metals.

KEY WORDS: (Ultra High Voltage E.B.) (Electron Beam Welding) (Weldability) (18%Ni Maraging Steel) (Hardness) (Impact Test) (Tensile Test) (COD Test)

1. Introduction

18%Ni maraging steel (HT 210) with extra low carbon content, which can attain tensile strengths of 190 to 210 kg/mm^2 after solution heat treatment and aging, possesses a superior strength-to-weight ratio and excellent fracture toughness, and thus is being increasingly used as a high tensile structural material in the most advanced technological fields, such as the aerospace industry, submarine applications, nuclear power, etc.[1),2)]. However, it is difficult to obtain satisfactorily strong and tough welds in maraging steels, because the strength and toughness of the welds depend strongly upon the welding processes, welding conditions and post-weld heat treatment conditions[2)]. TIG welding has so far been widely employed for maraging steels[3),4)], but because of multi-layer welding with high weld heat input, incompletely-hardened zones are observed in broad regions from the weld metals to the heat affected zones (HAZ) and moreover the grain growth occurs there, resulting in a decrease in strength; in addition, it is hard to change coarse grains into fine grains even by post-weld heat treatment. Consequently, in order to maintain high strength and toughness in weld metals and HAZ it is important to select a welding process which produces narrower incompletely-hardened zones, and appropriate heat treatments for achieving the best possible mechanical properties. In this regard, it is recommended that extremely narrow electron beam weld beads be constructed, in that the strength of the welded joint increases due to the plastic constraint of the base metal on the weld metal[5),6)].

Therefore, in this study, the welding of 18%Ni maraging steel HT 210 (hereinafter referred to as HT 210) was performed using a 300 kV ultra high voltage electron beam welder with a strong focusing electron beam gun with a 5 stage electromagnetic accelerating unit developed at the Arata Laboratory[7)], which is able to generate an extremely narrow ultra high energy density beam. First, the full penetration welding conditions for flat-position welding to assure narrow bead width and sound welds were determined. Furthermore, by the use of specimens of electron beam weld metals subjected to solution heat treatment and aging treatment, the effect of high temperature homogenization treatment on the mechanical properties was investigated and is discussed in terms of the reduction in the degree of solidification segregation and accordingly the disappearance of retained austenite (γ).

2. Electron Beam Welder, Materials Used and Experimental Procedure

An electron beam welder using a strong focusing

† Received on April 30, 1985
* Professor
** Associate Professor
*** Research Instructor

Transactions of JWRI is published by Welding Research Institute of Osaka University, Ibaraki, Osaka 567, Japan

electron beam gun with a 5 stage electromagnetic accelerating unit capable of generating an ultra high voltage of 300 kV was used for this experiment. **Figure 1** shows a general view of this welder.

The capacity of the welding chamber in this equipment is approximately 2 m^3.

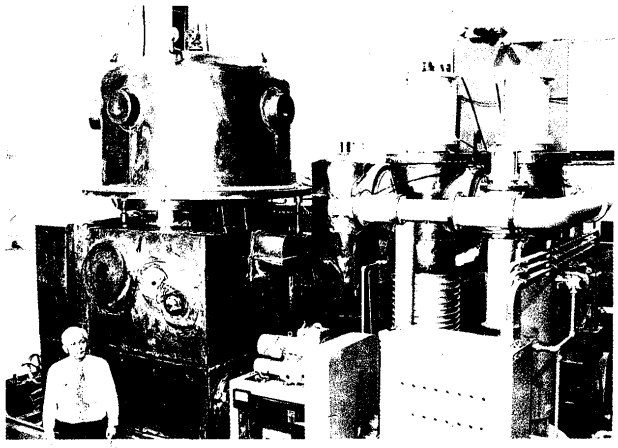

Fig. 1 General view of 300 kV, 100 kW E.B. welder with 5 stage electromagnetic accelerating unit gun.

The shapes of the high density beam in the welding chamber was investigated by the AB test method[8].

Figure 2 shows the beam shapes at the beam currents I_b = 20, 30, 40 mA when the beam voltage is constant at V_b = 250 kV.

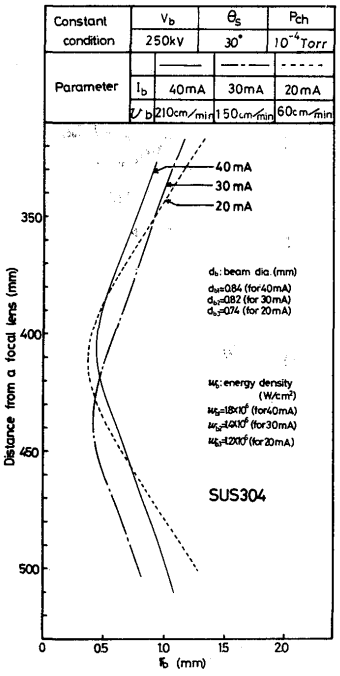

Fig. 2 Measurement results of E.B. shapes at various beam currents

18%Ni maraging steel (HT 210) plates of 12.8 mm thickness were used for this experiment. **Tables 1** and **2** show the chemical composition of HT 210 and its mechanical properties, respectively.

Flat position bead-on-plate welding was conducted. The welding conditions are shown in **Table 3**. **Table 4** shows combinations of the welding conditions used (beam current, welding speed and a_b value).

Table 1 Chemical composition of HT 210 (wt %)

C	Si	Mn	P	S	Ni	Cr	Co
0.002	0.01	0.02	0.002	0.001	18.14	0.1	8.5

Mo	Ti	Zr	B	Al	O	N
5.08	0.43	0.02	0.004	0.08	0.0015	0.0014

Table 2 Mechanical properties of HT 210 base metal

Tensile Strength (kg/mm^2)	V-notch impact value (kgm/cm^2)	K_{IC} ($kgf/mm^{3/2}$)
190 ∿ 215	≧ 2.0 (0°C)	≧ 225

Table 3 Welding conditions used in this investigation

Beam power	W_b=5 ∿ 10 kW
Beam voltage	V_b=250 kV
Beam current	I_b=20 ∿ 40 mA
Welding speed	υ_b=60 ∿ 240cm/min
a_b Value	a_b=0.75 ∿ 1.15
Deflect angle	θ_d= +10°
Chamber pressure	Pch=10^{-4} Torr

Table 4 Combinations of beam current, welding speed and a_b value

I_b (mA) \ a_b / υ_b (cm/min)	0.75				0.95							1.15			
	60	90	120	150	60	90	120	150	180	210	240	60	90	120	150
40	○	○	○	○	○	○	○	○	○	○	○	○	○	○	○
30	—	—	—	—	○	○	○	○	—	—	—	—	—	—	—
20	—	—	—	—	○	○	—	—	—	—	—	—	—	—	—

3. Solidification Cracking Susceptibility of HT 210

Hot cracking often occurs during the welding of high alloy steels with a high Ni content, and this constitutes a major problem. Since the HT 210 used for this experiment is a high alloy steel with 18%Ni content, its susceptibility to hot cracking during welding was examined. The Trans-Varestraint test[9),10)] was performed to quantitatively assess the high temperature ductility properties of the material during the solidification process. **Figure 3** shows the bead appearance of HT 210 weld metal with 2.5% strain applied. A number of cracks can be seen almost perpendicular to the ripple line corresponding to the back end of the weld puddle at the point where strain started to be applied. Particularly large cracks are apparent in the central part of the weld bead. The maximum length of the cracks which occurred near the center of the weld bead was measured, and the brittleness temperature range

(BTR) over which cracks occurred was calculated using the cooling curve during welding. The results are given in **Table 5**. The BTR for SUS 304 and SUS 310S (corresponding to AISI Type 304 and AISI Type 310S, respectively) are given for comparison[9),10)].

Judging from the BTR, when a low strain was applied, HT 210 seemed to have a slightly lower cracking susceptibility than SUS 310S, which is known as a material with high cracking susceptibility. If a high strain was applied, however, the cracking susceptibility became higher than that of SUS 310S and the possible occurrence of large cracks could be inferred. Thermal analysis results indicated that the melting point of HT 210 was approximately 1435°C, and so in order to prevent cracking it is necessary to select welding conditions which minimize the strains applied to solidifying weld metals and to keep the strain rates as slow as possible in the temperature range of approximately 1435°–1180° over which solidification cracks may occur[11)].

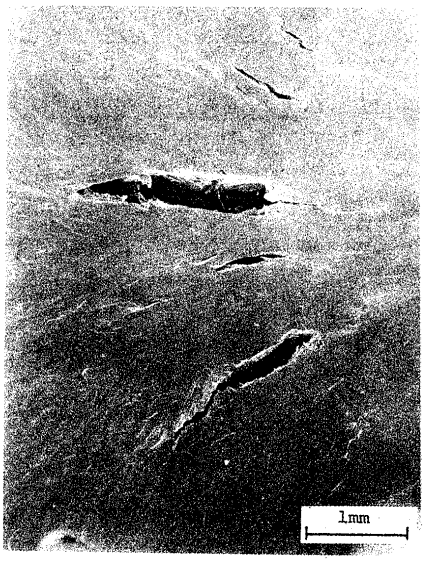

Fig. 3 Weld bead of HT 210 subjected to Trans-Varestraint test.

Table 5 BTR obtained by Trans-Varestraint test

Materials	ε(%)	BTR(°C)
HT 210	0.3	115
	0.5	208
	2.5	255
SUS 310S	0.3	125
	0.5	140
	2.5	160
SUS 304	0.5	65

4. Influence of Welding Conditions on Weld Bead Shape

It is desirable to make the weld bead width as narrow as possible in order to reduce the range of incomplete hardening (softening) in the weld metal and HAZ of HT 210[2),3)]. This means that the application of an ultra high density electron beam is advantageous because characteristic weld beads of deep penetration and narrow bead width can be easily produced.

The relationship between the power of an ultra-high voltage electron beam and its penetration properties was first examined by conducting partial penetration slope welding to determine welding conditions suitable for full penetration of 12.8 mm thick plate. **Figure 4** shows the cross sectional shape of a 30° down slope weld bead welded at beam power W_b=10 kW (V_b=250 kV, I_b=40

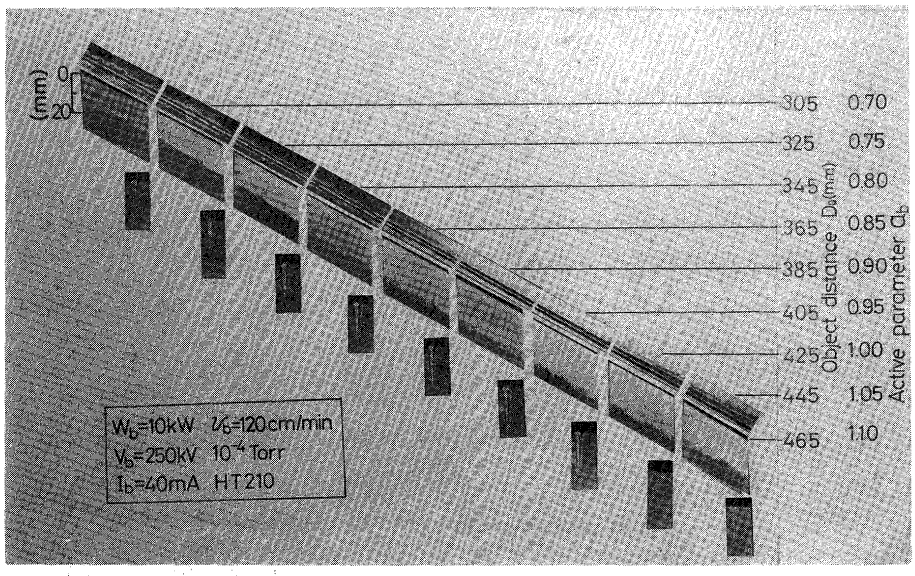

Fig. 4 Partially penetrated bead cross sections and appearance of down slope welding.

mA) and welding speed v_b=120 cm/min. In the range of a_b=0.90–1.10 (a_b value: objective distance/focal length) there is noticeable spiking, and at a_b=0.75–0.80 A-porosity (longitudinal cracking) occurs in the center of the bead. Penetration depth h_p is around 20 mm at about a_b=1, indicating the deep penetration characteristic of ultra high voltage electron beam welding. **Figure 5** shows the relationship between the a_b value and the penetration depth of HT 210 weld metals.

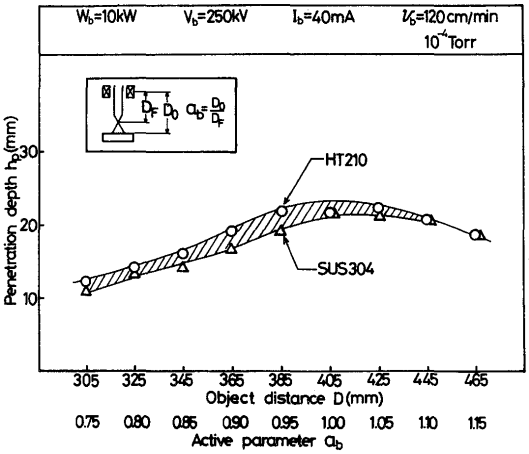

Fig. 5 Relationship between a_b value and penetration depth of HT 210 weld metals and, for comparison, SUS 304 weld metals.

Figure 6 shows SEM photographs of the longitudinal crack surface observed in the center part of the HT 210 bead produced at a_b=0.75–0.80. A characteristic dendritic crack surface is visible in the upper part of Fig. 6(a), while a crack surface of flat morphology is seen near the artificially fractured surface in the lower part of the picture. Fig. 6(b) shows an example of a crack surface seen elsewhere in higher magnification. Comparing these with crack surfaces produced by the Trans-Varestraint test, it is clear that these are solidification cracks. The above results confirm that great care should be taken in E.B. welding of HT 210 to select welding conditions which will not give rise to various defects.

Figure 7 shows fully penetrated bead cross sections and bead appearances for 12.8 mm plates of HT 210 made at welding speeds v_b=90, 150 and 210 cm/min (a_b=0.95, W_b=10 kW, V_b=250 kV).

An extremely small amount of reinforcement can be seen on the bead surface in full penetration welding of HT 210. This is attributed to the disappearance of the weld metal necessary for reinforcement through spattering from the molten pool and flowing of the molten metal out of the beam hole in the underside of the bead. How-

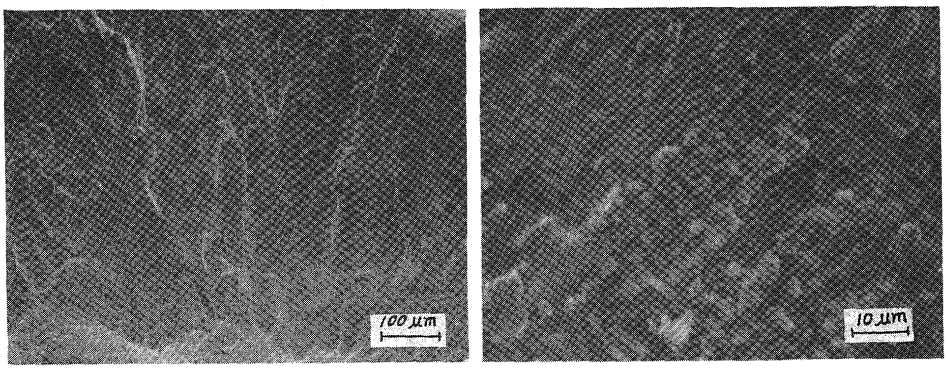

(a) (b)

Fig. 6 SEM photographs of solidification crack surfaces.
(V_b=250 kV, I_b=40 mA, v_b=60 cm/min, a_b=0.75)

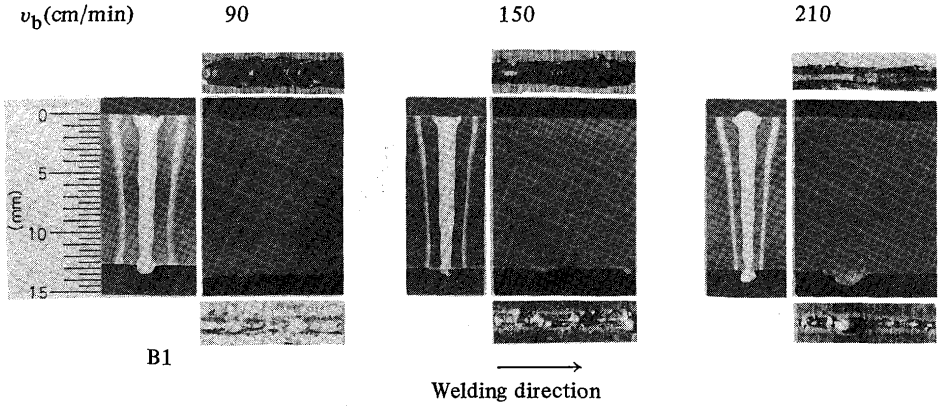

W_b = 10kW V_b = 250kV I_b = 40mA a_b = 0.95 10^{-4} Torr HT210

Fig. 7 Fully penetrated bead cross sections and appearances of flat position weld metals at various welding speeds

ever, good beads without weld defects were obtained despite large changes in v_b. Thereafter, a well-type bead with a parallel practical bead width d_B of approximately 1.5 mm (as shown in Fig. 7) was used as welding condition B1 for an examination of the metallurgical and mechanical properties of the weld metal.

Figure 8 shows the bead width (d_{B0}, $d_{B1/2}$, d_{B1}) with variation in the welding speed at W_b = 10 kW. Bead width decreased with an increase in the welding speed from 60 to 180 cm/min, and at v_b = 210 cm/min a "vermicular" pass (partial, not through) bead with a wide bead surface was observed.

Figure 9 shows fully penetrated bead cross sections and external views of HT210 welded at W_b = 10 kW and v_b = 120 cm/min with a_b = 0.75, 0.95 and 1.15. It is apparent that surface bead width and accordingly the bead shape varied with the a_b value. When the a_b value was 0.75 or 1.15, the beads became broad, curved, wedge-type beads, and even in this kind of bead there were no weld defects.

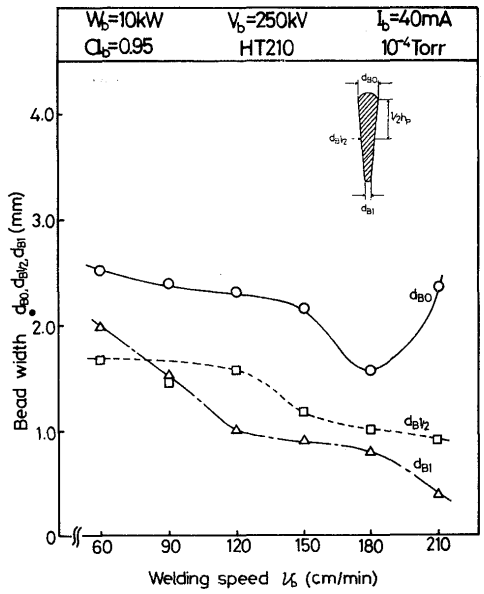

Fig. 8 Relation between bead width and welding speed in full penetration welding.

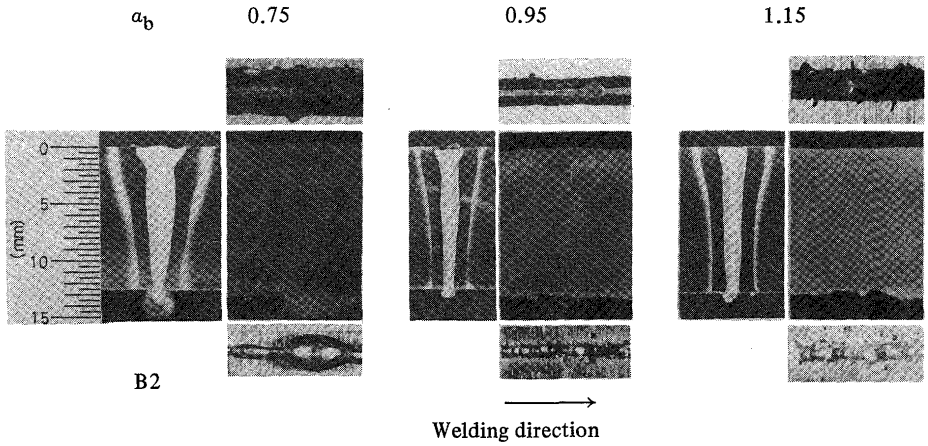

W_b = 10kW V_b = 250kV I_b = 40mA v_b = 120(cm/min) 10^{-4} Torr HT210

Fig. 8 Fully penetrated bead cross sections and appearances of flat position weld metals at various a_b values

This wedge-type bead at a_b = 0.75 with a practical bead width of approximately 2.1 mm (as shown in Fig. 8) was adopted as welding condition B2.

In addition, the $\mathscr{I}$ value (beam pass ratio = pass current/incident beam current x 100) was also measured. The $\mathscr{I}$ value was 35, 20 and 8% at v_b = 60, 120 and 180 cm/min, respectively, decreasing as the welding speed increased. On the other hand, in the case of wedge-type B2 bead at a_b = 0.75, the $\mathscr{I}$ value was 4 ~ 5%, which was quite small.

5. Microstructural Features of E.B. Welds and Hardness Distribution in Welds

The correlation among the welding conditions, the microstructure of HT 210 welds and the distribution of hardness was investigated with the objective of finding out the decisive factors for setting the suitable welding parameters and heat-treatment conditions.

In the initial stage, the solution heat treatment at 830°C x 1 hr, which is commonly employed on the welds of HT 210, was carried out[3]. This heat treatment temperature was found to be below the recrystallization temperature of HT 210 weld metals, leaving the weld metals with some incompletely-hardened zones. The cause of such incompletely-hardened zones was studied from the standpoint of solidification segregation and retained austenite (γ), and at the same time solution heat treatment, which is designed to dissipate such zones, was examined to further improve the microstructure and hardness.

5-1 Effect of welding conditions on microstructure

Incomplete hardening (softening) due to the formation of retained γ takes place in electron beam weld metals. In order to reduce the harmful effect of incomplete harden-

ing on strength and toughness and promote the disappearance of the γ phase in treatment, it is important to select welding conditions which result in a narrow weld bead width, minimize the width of the incompletely hardened zones[12] and produce a small cell size in the microstructure.

Figure 10 shows the optical as-weld microstructures of welds under welding conditions B1 and B2 (B1: well-type bead at W_b=10 kW, v_b=90 cm/min and a_b=0.95; B2: wedge-type bead at W_b=10 kW, v_b=120 cm/min and a_b=0.75). Grains which are not very coarse are observed in the HAZ near the bonds under both conditions. The

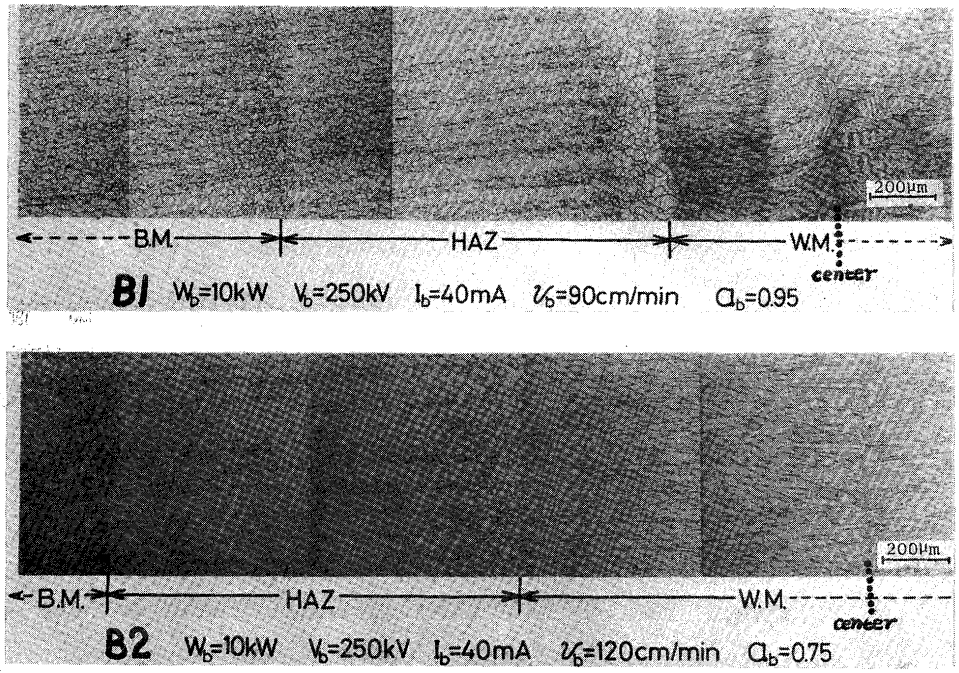

Fig. 10 Microstructures of HT 210 welds under welding conditions B1 and B2

weld metal under welding condition B2 shows cellular dendrites growing from the bonds and crushing against each other almost on the bead center line. **Figure 11** shows a Nomarsky polarization microstructure near the bond of the HT 210 welds under welding condition B1, presenting clearer grain boundaries. The bonds show epitaxial growth[13] and an extremely narrow planar growth, which immediately indicates the growth of cells or cellular dendrites. The narrow cell width of about 1.25 μm demonstrates that the electron beam welds cooled rapidly, suggesting why the grains did not become coarse in HAZ. Similar structures could also be seen under B2 conditions.

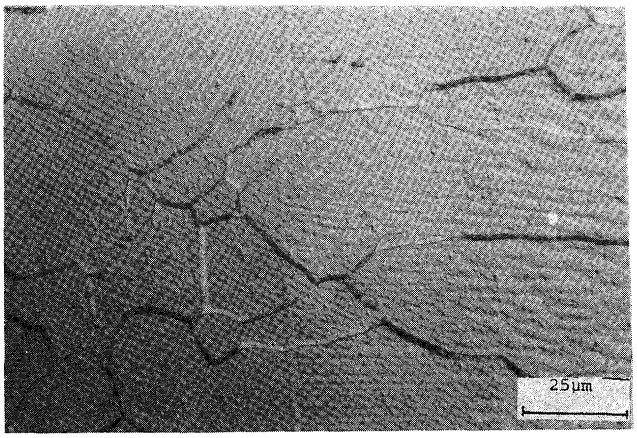

Fig. 11 Microstructure near the bond of HT 210 weld showing grains in HAZ and cell boundaries in weld metal.

5.2 Effect of solution treatment temperature on hardness

Table 6 Heat Treatment Conditions

	Heat treatment condition
S1	830°CX1hr A.C. 485°CX5hr A.C.
S2	1100°CX1hr A.C. 850°CX1hr A.C. 485°CX5hr A.C.

Table 6 shows heat treatment conditions used for this study. In S1, standard solution treatment was carried out near the recrystallization temperature of 830°C×1 hr under the same heat treatment conditions as those currently employed for HT 210 base metals. In S2, solution treatments were performed especially at both 1100°C×1 hr to reduce segregation of the alloying elements and at 850°C×1 hr to achieve grain-refinement. S1 and S2 also include aging treatment at 485°C×5 hrs.

Figure 12 shows the Vickers hardness distribution of HT 210 under the B1 welding parameters for varying

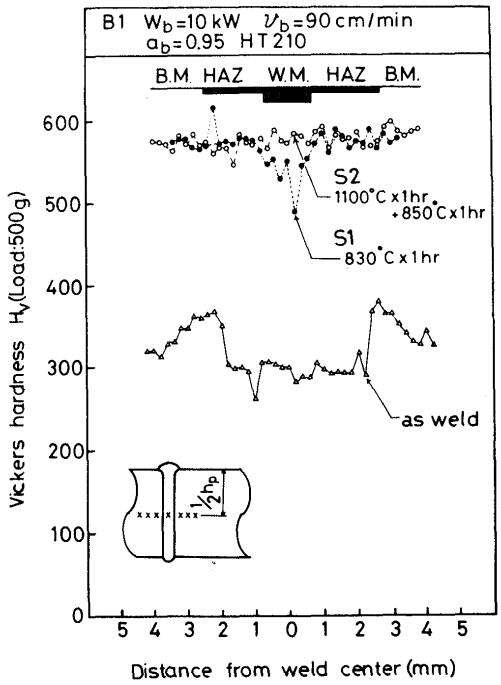

Fig. 12 Hardness distribution of HT 210 welds for the two solutions under welding condition B1.

solution treatment conditions. For as-weld, the Vickers hardness (Hv) of the weld metals and HAZ is about 300, except for a maximum hardness of about 380 in HAZ near the base metal. For S1 treatment, the Hv of the base metal and HAZ is 560-580 and the weld metal shows the formation of incompletely-hardened zones of about 500 Hv. After S2 treatment at 1100°C, the hardness of the weld metal shows an increase similar to that of the base metal, and no incompletely-hardened zones can be seen. Under B2 welding conditions, almost similar trends were observed, although bead width was slightly greater.

From the above results it was concluded that normal S1 heat treatment at 830°C x 1 hr produced incompletely-hardened zones in weld metals and the treatment temperature was too low to reduce solidification segregation in electron beam weld metals. Moreover, it was revealed that the hardness of the weld metals improved to the same level as the base metal by subjecting them to S2 treatment at 1100°C x 1 hr.

5.3 Solidification segregation and retained austenite in weld metals

The formation of incompletely hardened zones in electron beam weld metals was considered to be due to solidification segregation because major alloying elements contributing to hardening were reduced in cell cores, leading to lesser hardening, and because at solidification grain boundaries and cellular dendritic boundaries alloying elements were increased to such an extent that Ms points decreased and consequently soft γ was retained.

In order to clarify the correlation between solidification segregation and the formation of the residual γ phase, SEM observations of the microstructures and element analyses were made in weld metals using an energy dispersive X-ray spectrometer (EDX). Thus, residual γ content was measured by joint use of optical examination and X-ray diffraction[14,15].

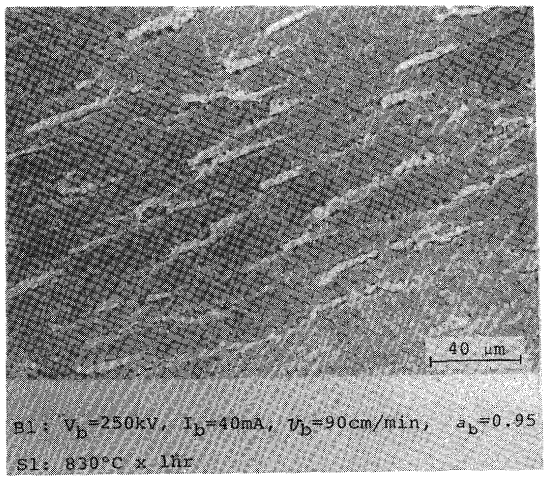

Fig. 13 SEM photograph of HT 210 weld metal after S1 treatment at 830°C x 1 hr.

Figure 13 is a SEM photo of weld metal after S1 treatment under welding condition B1. The microstructure shows traces of solidification grain boundaries and cell boundaries, with either granular or elongate white phase scattered along these boundaries. The area percentage of this white phase was measured and found to be about 10%. This white phase, according to the results of X-ray diffractometer measurements, was identified as residual γ phase.

The results of EDX spot analyses of cell cores and the white γ phase suggest that the white γ phase, as compared to cell cores, presents higher peak values in both Mo and Ti. **Figure 14**(a) is a summary of the EDX spot analysis results across the cell from the cell core to the white γ phase. For each element the marks indicate the relative intensity obtained by dividing the count for each element by the total count for Fe, Ni, Co, Mo and Ti. As for Co and Ni, these values include the counts of $Fe_{K\beta 1}$ and $Co_{K\beta 1}$, respectively. The result in Fig. 14(a) clearly shows the white γ phase to be enriched in Mo and Ti and depleted in Fe. Fig. 14(b) shows an example of the X-ray diffractometer results in identifying the microconstituents of weld metals. By analyzing the large peak in the α' phase and the small peak in the γ phase, the residual content obtained was about 11%, which is in good agreement with the above-mentioned result obtained by SEM observation.

The retained γ seems to have been formed because solidification segregation was not removed by S1 treat-

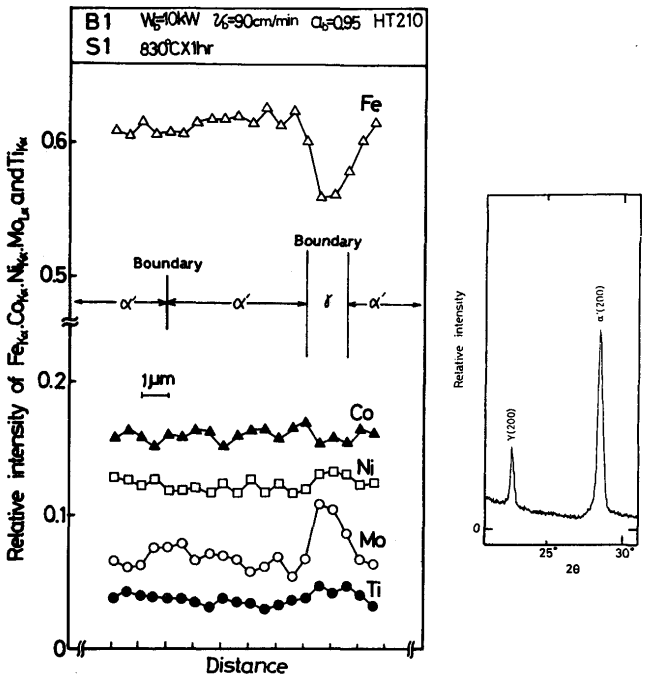

(a) (b)

Fig. 14 Results of EDXanalysis (a) and X-ray diffraction profile (b) of HT 210 electron beam weld metal (solution condition: 830°C x 1 hr).

ment at 830°C for 1 hr. Therefore, the solidification segregation and the residual γ content in as-weld metals were investigated by means of EDX analysis and X-ray diffraction methods. **Figure 15**(a) shows the EDX analysis results of the well-type beads under welding condition B1. It is confirmed that Mo and Ti are liable to segregate in relation to the decrease in relative intensity of Fe at the solidification boundaries. According to the results of X-ray diffraction shown in Fig. 15(b), the residual γ content reached 15 to 16%, which is slightly higher than the γ content after S1 treatment. **Figure 16** (a) & (b) show the results of EDX analysis and X-ray diffraction after S2 treatment of a homogenized bead under welding condition B1. S2 solution treatment has successfully removed the residual γ phase, as well as solidification segregation.

It was found from all the above results that Mo and Ti were segregated at the solidification boundaries and cell boundaries, and thereby about 10% or so of γ phase remained at the boundaries after welding. Moreover, although S1 treatment (830°C x 1 hr) could not successfully remove the γ phase, S2 treatment (1100°C x 1 hr and 850°C x 1 hr) almost completely decreased the degree of segregation, and thus succeeded in eliminating the residual γ phase. This accounts for the fact that S2 treatment improved the hardness of the weld metals to the same level as the base metals.

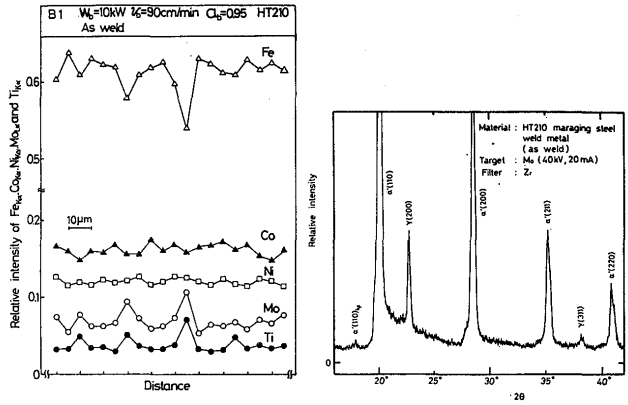

(a) (b)

Fig. 15 Results of EDX analysis (a) and X-ray diffraction (b) of HT 210 electron beam weld metal.

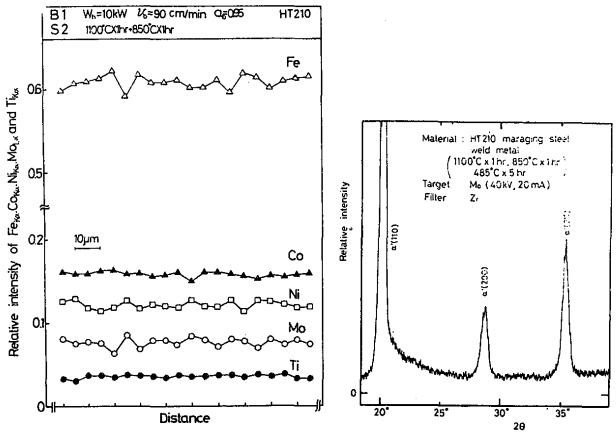

(a) (b)

Fig. 16 Results of EDX analysis (a) and X-ray diffraction (b) of HT 210 electron beam weld metal (solution: 1100°C x 1 hr and 850°C x 1 hr).

6. Mechanical Properties of E.B. Welded Joints

Welded joints were subjected to impact, tensile and COD tests in order to clarify the effects of the welding conditions and solution heat treatment conditions on their mechanical properties. The results are shown below.

6.1 Impact test

For impact testing the V-noched Charpy impact test was employed, using JIS-4 specimens machined from the center part of a 12.8 mm thick plate. **Table 7** shows the test results at 0°C for combinations of welding conditions B1 and B2 and solution treatment conditions S1 and S2 (impact values are the means of five specimens). All combinations produced values exceeding 2.0 (kg/cm^2), which is required for base metals of HT 210.

Table 7 Results of Charpy impact test of HT 210 (at 0°C)

Welding condition / Solution	B1	B2
S1: 830°C x 1 hr	(kgm/cm²) 2.3	(kgm/cm²) 2.3
S2: 1100°C x 1 hr +850°C x 1 hr	2.3	2.7

6.2 Tensile test

The tensile strength of welded joints was studied using the specimens shown in **Figure 17**. Testing was performed on a 50-ton universal tensile test machine.

Table 8 shows the results of room temperature tensile tests. Under both welding conditions B1 and B2, S2 treatment tended to produce higher tensile strength than S1.

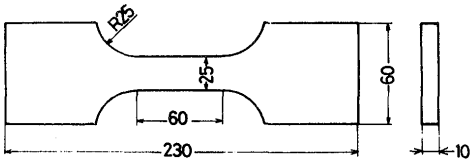

Fig. 17 Dimensions of tensile test specimen

Table 8 Results of welded joint tensile test (at room temperature)

	Welding condition	Solution	Tensile strength (kg/mm²)	Elongation	Fractured point
1	B1	S1: 830°C x 1 hr	196.3	8.5	WM + HAZ
2			197.7	9.0	WM + HAZ
3		S2: 1100°C x 1 hr +850°C x 1 hr	201.9	8.5	BM
4			201.1	8.5	WM + HAZ
5	B2	S1: 830°C x 1 hr	196.4	10.0	WM + HAZ
6			196.7	12.0	WM + HAZ
7		S2: 1100°C x 1 hr +850°C x 1 hr	201.6	10.0	BM
8			199.6	7.5	BM

Table 9 shows the results of the tests. For S1 treatment, the K_{IC} value of the weld metal was below 225 (kg/mm$^{3/2}$), the required value for the base metal, presumably due to the influence of the residual γ phase. The values obtained for S2 treatment satisfy the requirements, achieving a clear improvement in the K_{IC} value.

Table 9 Results of COD test

Solution	K_{IC} (kg/mm$^{3/2}$)			
	B1		B2	
	Weld metal	HAZ	Weld metal	HAZ
S1: 830°C x 1 hr	205.6	293.0	182.5	316.4
S2: 1100°C x 1 hr +850°C x 1 hr	238.8	290.9	275.3	287.9

Values obtained for all cases satisfied the requirements for base metals: 190-215 (kg/cm²). The satisfactory strength of E.B. weld metals is attributed to the narrow weld beads produced by ultra-high voltage E.B. welding.

6.3 COD test

Three-point bending COD testing (support distance: 80 mm) was carried out on specimens with a 0.2 mm saw-cut notch tip, according to ASTM E 399, as shown in **Figure 18**.

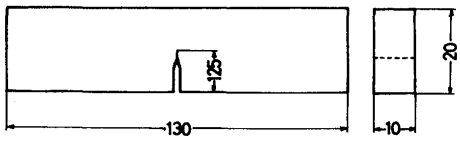

Fig. 18 Dimensions of COD test specimen

7. Conclusions

A study of the applicability of an ultra high energy density heat source to flat-position full-penetration welding in 18%Ni maraging steel (HT 210) suceeded in obtaining a good sound weld bead without any defects over a wide range of welding conditions. Moreover, the phenomenon of incomplete hardening of the weld metals could be improved by eliminating solidification segregation and retained γ phase responsible for such incomplete hardening, by performing homogenization solution heat treatment at 1100°C. A combination of homogenization solution treatment and grain-refining solution heat treatment at 850°C resulted in substantial improvement in both the hardness and fracture toughness.

Acknowledgements

The financial support for this study from the Ministry of Education is gratefully acknowledged. The authors wish to thank Prof. Dr. R. Horiuchi, Professor of the Institute of Space and Astronautical Science, for his intensive valuable discussion and also would like to acknowledge Mitsubishi Heavy Industries, Ltd. for supplying materials and performing some tests. Special thanks are also expressed to Mr. M. Yakeno, former graduate student, for his cooperation in conducting experimental work.

References

1) S. Sato and H. Ono: Metals, Vol. 44 (1974), No. 8, 40 (in Japanese).

2) Y. Kawabe: Bulletin of The Japan Institute of Metals, Vol. 14 (1975), No. 10, 767 (in Japanese).

3) K. Hosomi, O. Tsutsumi and Y. Ashida: Kobe Steel Engineering Reports (R&D), Vol. 21 (1971), No. 4, 12 (in Japanese).

4) Y. Kawabe, M. Kanao, S. Muneki and K. Nakano: Tetsu-to-Hagane (Journal of the Iron and Steel Institute of Japan), Vol. 59 (1973), No. 9, 1328 (in Japanese).

5) K. Satoh and M. Toyoda: Journal of The Society of Naval Architects of Japan, 431 (1973), 355 (in Japanese).

6) S. Nishida, H. Yada and H. Yamamoto: Journal of JWS, Vol. 44 (1975), No. 6, 451 (in Japanese).

7) Y. Arata and M. Tomie: Journal of JWS, Vol. 46 (1977), No. 8, 429 (in Japanese).
Y. Arata and M. Tomie: Journal of High Temperature Society, Vol. 10 (1984), No. 3, 110 (in Japanese)
Y. Arata, M. Tomie, H. Otera, S. Noguchi and Y. Yakeno: Research Committee for Welding JWS, No. EBW-294-82, (1982), (in Japanese).

8) Y. Arata, M. Tomie, K. Terai, H. Nagai and T. Hattori: Trans. of JWRI, Vol. 2 (1973), No. 2, 1., IIW Doc. IV-114-73 (1973).
Y. Arata: IIW Doc. IV-340-83 (1983).

9) Y. Arata, F. Matsuda and S. Katayama: Trans. of JWRI, Vol. 6 (1977), No. 1, 105.

10) S. Katayama: Doctor thesis, Osaka University, Oct. 1981 (in Japanese).

11) Y. Arata, F. Matsuda, H. Nakagawa, S. Katayama and S. Ogata: Trans. of JWRI, Vol. 6 (1977), No. 2, 197

12) M. Fujita, Y. Kawabe, H. Irie and S. Tsukamoto: Tetsu-to-Hagane (J. of ISIJ), Vol. 69 (1983), No. 8, 990 (in Japanese).

13) W.F. Savage, C.D. Lundin and A.H. Aronson: Welding Journal, Vol. 44 (1965), No. 4, 175-s.

14) B.D. Cullity: "Elements of X-Ray Diffraction", Addison-Wesley Publishing Co., Inc., Massachusetts.

15) R.L. Miller: Trans. ASM, Vol. 57 (1964), 892.